

Error Probability Expressions for Frame Synchronization Using Differential Correlation

Sangtae Kim, Jaewon Kim, Dong-Joon Shin, Dae-Ig Chang, and Wonjin Sung

Abstract: Probabilistic modeling and analysis of correlation metrics have been receiving considerable interest for a long period of time because they can be used to evaluate the performance of communication receivers, including satellite broadcasting receivers. Although differential correlators have a simple structure and practical importance over channels with severe frequency offsets, closed-form expressions for the output distribution of differential correlators do not exist. In this paper, we present detection error probability expressions for frame synchronization using differential correlation, and demonstrate their accuracy over channel parameters of practical interest. The derived formulas are presented in terms of the Marcum Q -function, and do not involve numerical integration, unlike the formulas derived in some previous studies. We first determine the distributions and error probabilities for single-span differential correlation metric, and then extend the result to multi-span differential correlation metric with certain approximations. The results can be used for the performance analysis of various detection strategies that utilize the differential correlation structure.

Index Terms: Differential correlation, false alarm rate, frame synchronization, mis-detection probability, satellite transmission.

I. INTRODUCTION

Broadcasting services via satellite transmission are being provided to an increasing number of users, and new standards with enhanced transmission capabilities are being developed. For example, the second-generation digital video broadcasting for satellites (DVB-S2), has incorporated new technical features so that high-quality broadcasting services can be provided [1]–[3]. However, several challenges are involved in the implementation of a system with advanced transmission capabilities. The DVB-S2 standard requires receiver operation at sub-zero signal-to-noise ratios (SNR); this is enabled by the powerful error-correction capability of low-density parity-check (LDPC) codes. Thus, carrier recovery may be more difficult when a certain level of phase noise is present in consumer low noise block (LNB) converters and tuners. The synchronization of DVB-S2 receivers must also cope with the wide range of possible system configurations and the presence of operative modes

working at very low SNRs, in addition to large frequency offsets [3], [4]. Under such circumstances, the development of robust synchronization methods and the exact identification of their performance becomes very important.

Initial acquisition using frame synchronization has been a topic of both theoretical analysis and practical development. The seminal work by Massey presented an optimal correlator for coherent detection based on the maximum likelihood (ML) statistics [5]. This correlation scheme was subsequently extended to specific modulation methods and approximated to obtain suboptimal solutions [6]–[9]. For coherent correlators, closed-form expressions for the error probabilities are known [10]. Synchronization using coherent correlation, however, causes considerable degradation in performance when frequency offsets due to the Doppler shift or oscillator frequency drift exist in the channel.

To circumvent the effects of frequency offsets, various synchronization methods and their performance in different channel environments have been studied. Although some of the methods use the partial correlation properties of synchronization sequences [11] and noncoherent combinations of the correlation over subintervals [12], many other schemes are based on differential correlation [13]–[20]. In particular, the detection methods in [13] are derived from approximated ML metrics to provide robust synchronization performance under frequency offsets. To reduce the complexity of the synchronization operation, appropriate adjustments to the differential correlator structure have been made and the corresponding performance has been investigated [14]–[17]. These schemes in general use limited “spans” for the differential correlation and produce an efficient tradeoff between performance and complexity. Analyses of the differential detection for pseudo-random code acquisition are described in [18] and [19].

Although differential-correlation-based synchronization methods are widely used, the results for the related statistical analysis and the derivation of the error probability expressions are not as well known as those for their coherent counterparts. There are several reasons for this, including the complication due to the noise product term and the strong correlations among the variables constituting the decision metric. Due to these reasons, existing analytic results either exhibit inaccuracy arising from approximations or contain expressions involving numerical integrations. Discussions of the statistical distributions relating to differential correlation can be found in [20] as well as in the aforementioned references [13]–[19].

The main purpose of this paper is to present the analytic expressions for the error probabilities as well as the statistical distributions for the differential-correlation decision metric, when the frame synchronization is performed over the additive white

Manuscript received April 06, 2010.

This work is supported by the IT R&D program of KCC/IITA 2008-S008-02, Development of 21GHz Band Satellite Broadcasting Transmission Technology, and in part by the Special Research Grant of Sogang University.

S. Kim, J. Kim, and W. Sung are with the Department of Electronic Engineering, Sogang University, Seoul, 121-742, Korea, email: {rlatkdxo80, jaewonkim, wsung}@sogang.ac.kr.

D.-J. Shin is with the Department of Electronic Engineering, Hanyang University, Seoul, 133-791, Korea, email: djshin@hanyang.ac.kr.

D.-I. Chang is with Electronics and Telecommunications Research Institute, Daejeon, 305-700, Korea, email: dchang@etri.re.kr.

Gaussian noise (AWGN) channel. In contrast to some previous results, our expressions do not involve numerical integration, which complicates the evaluation, and the accuracy of the formulas is verified for a wide range of channel conditions. The results can also be used for further performance evaluation and analysis of various forms of frame synchronization that include the differential correlation structure. This paper is organized as follows. The signal model and the differential correlator structure for performance analysis are introduced in Section II. In Section III, the statistical distributions for the differential correlated metric are determined by decomposing the metric into parts. Both the misdetection probability (MDP) and the false alarm rate (FAR) are determined using the derived cumulative distribution functions (CDF). Generalization to the case in which the correlation involves multiple symbol spans is discussed in Section IV, and the numerical verification of the formulas is given in Section V. The conclusions are presented in Section VI.

II. SIGNAL AND CORRELATOR MODELS

We consider the continuous transmission of data frames over the AWGN channel. Each frame consists of a synchronization sequence of L consecutive symbols followed by $N - L$ data symbols, as shown in Fig. 1. After performing perfect symbol-time synchronization, the received sample at the m th symbol time can be written as

$$r_m = s_m e^{j(2\pi m f_0 T_s + \phi_0)} + n_m \quad (1)$$

where s_m is the transmitted symbol with normalized power $E\{|s_m|^2\} = 1$ and n_m is the zero-mean complex white Gaussian noise sample with variance σ_n^2 for both in-phase and quadrature components. Parameters f_0 and ϕ_0 represent the unknown frequency and phase offsets, respectively, and T_s represents the symbol period. We assume that f_0 takes one of the values from $[-f_{max}, +f_{max}]$ where f_{max} represents the maximum frequency offset, and ϕ_0 takes one of the values from $[-\pi, +\pi]$.

Frame synchronization using differential correlation performs the correlation of the L consecutive samples with the synchronization sequence symbols d_0, d_1, \dots, d_{L-1} in the form of $\sum_{i=1}^{L-1} r_{i+m}^* d_i r_{i+m-1} d_{i-1}^*$ [13]. For notational simplification, we drop the symbol index by letting $m = 0$ without loss of generality and define

$$Y = \sum_{i=1}^{L-1} r_i^* d_i r_{i-1} d_{i-1}^*. \quad (2)$$

The corresponding *differential correlation metric* uses its squared magnitude

$$S = |Y|^2. \quad (3)$$

The differential correlation in (2) can be generalized to the *k-span differential correlation* defined as

$$Y(k) = \sum_{i=k}^{L-1} r_i^* d_i r_{i-k} d_{i-k}^*. \quad (4)$$

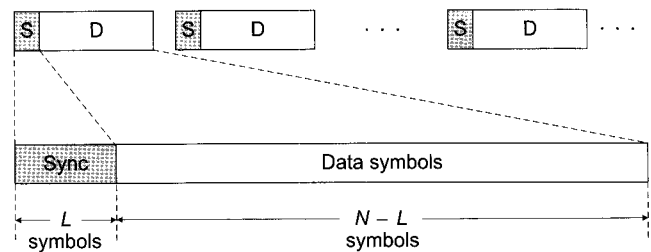


Fig. 1. Continuous transmission of frames of N symbols. Each frame includes the synchronization sequence of L symbols in its header.

The correlation metric that uses the squared magnitudes of k -span differential correlation summed from $k = 1$ to a predetermined parameter K , referred to as the *multi-span differential correlation metric*, is expressed as

$$S = \sum_{k=1}^K |Y(k)|^2. \quad (5)$$

Although the value of K can be as large as $L - 1$, an appropriate small value is usually chosen to control the complexity of the detection without significantly sacrificing performance [14]. We first determine the statistical distributions of the differential correlation metric in (3); they are subsequently extended to distributions for the multi-span metric in (5). For notational simplicity, our analysis is based on quadrature phase shift keying (QPSK) modulated symbols chosen from the signal constellation $\{1, j, -1, -j\}$ with equal probability. However, with straightforward modifications, the derivation procedure described in this paper is directly applicable to any other phase shift keying (PSK) as well as to amplitude phase shift keying (APSK) modulation types. The QPSK results reported in this paper can be easily extended to other modulation types by simply changing the equation coefficients. This simple extension is possible since all the distributions derived including the weighted sum of Gaussian, chi-square, and binomial random variables are valid for both PSK and APSK modulations.

In the following, subscripts I and Q denote the in-phase and quadrature components, respectively, of a given variable, e.g., $Z_I = \Re\{Z\}$ and $Z_Q = \Im\{Z\}$ for complex random variable Z , where $\Re\{\cdot\}$ and $\Im\{\cdot\}$ represent the real and imaginary parts. The expectation, variance, and covariance are denoted by $E\{\cdot\}$, $Var\{\cdot\}$, and $Cov\{\cdot, \cdot\}$, respectively. A real random variable R following the Gaussian distribution with mean μ and variance σ^2 is denoted by $R \sim N(\mu, \sigma^2)$.

III. DIFFERENTIAL CORRELATION STATISTICS

We investigate the distribution of the differential correlation metric in (3) for both the synchronous and asynchronous cases. In the synchronous case H_1 , the correlation is performed over the received data, which exactly correspond to the synchronization sequence, so we have $s_i = d_i$ for $i = 0, 1, \dots, L - 1$. The asynchronous case H_0 refers to all other correlations, and $s_i \neq d_i$ for $i = 0, 1, \dots, L - 1$. Combining (1) and (2) gives

$$Y = \sum_{i=1}^{L-1} (s_i e^{j(2\pi i f_0 T_s + \phi_0)} + n_i)^* d_i$$

$$\begin{aligned} & \times (s_{i-1}e^{j(2\pi(i-1)f_0T_s+\phi_0)} + n_{i-1})d_{i-1}^* \\ & = e^{-j2\pi f_0T_s} \left[\sum_{i=1}^{L-1} s_i^* s_{i-1} d_i d_{i-1}^* + \sum_{i=1}^{L-1} s_i^* \tilde{n}_{i-1} d_i d_{i-1}^* \right. \\ & \quad \left. + \sum_{i=1}^{L-1} \tilde{n}_i^* s_{i-1} d_i d_{i-1}^* + \sum_{i=1}^{L-1} \tilde{n}_i^* \tilde{n}_{i-1} d_i d_{i-1}^* \right] \quad (6) \end{aligned}$$

where we defined $\tilde{n}_i \triangleq n_i e^{-j(2\pi i f_0 T_s + \phi_0)}$. Note that \tilde{n}_i is simply a phase-rotated version of n_i and follows the identical distribution. We further define four separate terms in the square bracket of (6) as

$$U \triangleq \sum_{i=1}^{L-1} s_i^* s_{i-1} d_i d_{i-1}^*, \quad (7)$$

$$V \triangleq \sum_{i=1}^{L-1} s_i^* \tilde{n}_{i-1} d_i d_{i-1}^*, \quad (8)$$

$$W \triangleq \sum_{i=1}^{L-1} \tilde{n}_i^* s_{i-1} d_i d_{i-1}^*, \quad \text{and} \quad (9)$$

$$X \triangleq \sum_{i=1}^{L-1} \tilde{n}_i^* \tilde{n}_{i-1} d_i d_{i-1}^*. \quad (10)$$

Using these definitions, the metric S in (3) can be written as

$$S = |U + V + W + X|^2 = |\tilde{Y}|^2 \quad (11)$$

where $\tilde{Y} \triangleq U + V + W + X$.

A. Synchronous Case

The distribution of S can be derived using individual distributions for U , V , W , and X . For the synchronous case, we have $s_i = d_i$ and variable U in (7) becomes

$$U = L - 1. \quad (12)$$

Further, variables V and W become $V = \sum_{i=1}^{L-1} \tilde{n}_{i-1} d_i^*$ and $W = \sum_{i=1}^{L-1} \tilde{n}_i^* d_i$, i.e.,

$$V = \tilde{n}_0 d_0^* + \cdots + \tilde{n}_{L-2} d_{L-2}^* \quad (13)$$

and

$$W = \tilde{n}_1^* d_1 + \cdots + \tilde{n}_{L-1}^* d_{L-1}. \quad (14)$$

Each term in the RHS of (13) and (14) is obtained by the phase rotation of the noise sample and follows the identical distribution $N(0, \sigma_n^2)$. Since $\Re\{\tilde{n}_i d_i^*\} = \Re\{\tilde{n}_i^* d_i\}$, the sum of the in-phase components of V and W is

$$V_I + W_I = \Re\{\tilde{n}_0 d_0^*\} + \Re\{\tilde{n}_{L-1} d_{L-1}^*\} + 2 \sum_{i=1}^{L-2} \Re\{\tilde{n}_i d_i^*\} \quad (15)$$

which is the sum of real Gaussian variables. Hence, $V_I + W_I$ is also Gaussian with mean $E\{V_I + W_I\} = 0$ and variance $Var\{V_I + W_I\} = (2 + 4(L-2))\sigma_n^2$. The sum of the quadrature components of V and W becomes

$$V_Q + W_Q = \Im\{\tilde{n}_0 d_0^*\} + \Im\{\tilde{n}_{L-1}^* d_{L-1}\} \quad (16)$$

using the relation $\Im\{\tilde{n}_i d_i^*\} = -\Im\{\tilde{n}_i^* d_i\}$, and $V_Q + W_Q$ follows the Gaussian distribution with mean $E\{V_Q + W_Q\} = 0$ and $Var\{V_Q + W_Q\} = 2\sigma_n^2$. These observations are summarized by

$$V_I + W_I \sim N(0, (4L-6)\sigma_n^2) \quad (17)$$

and

$$V_Q + W_Q \sim N(0, 2\sigma_n^2). \quad (18)$$

For variable $X = \sum_{i=1}^{L-1} \tilde{n}_i^* \tilde{n}_{i-1} d_i d_{i-1}^*$, each element $\tilde{n}_i^* \tilde{n}_{i-1} d_i d_{i-1}^*$ in the summation is a phase-rotated version of $\tilde{n}_i^* \tilde{n}_{i-1}$ and hence it suffices to inspect its distribution. The real and imaginary parts of $\tilde{n}_i^* \tilde{n}_{i-1}$ are

$$\Re\{\tilde{n}_i^* \tilde{n}_{i-1}\} = \Re\{\tilde{n}_i^*\} \Re\{\tilde{n}_{i-1}\} - \Im\{\tilde{n}_i^*\} \Im\{\tilde{n}_{i-1}\} \quad (19)$$

and

$$\Im\{\tilde{n}_i^* \tilde{n}_{i-1}\} = \Re\{\tilde{n}_i^*\} \Im\{\tilde{n}_{i-1}\} + \Im\{\tilde{n}_i^*\} \Re\{\tilde{n}_{i-1}\}. \quad (20)$$

It immediately follows that $E\{\Re\{\tilde{n}_i^* \tilde{n}_{i-1}\}\} = 0$ and

$$Var\{\Re\{\tilde{n}_i^* \tilde{n}_{i-1}\}\} = E\{(\Re\{\tilde{n}_i^* \tilde{n}_{i-1}\})^2\} = 2\sigma_n^4 \quad (21)$$

holds. The mean and variance of the in-phase component of X are determined as

$$E\{X_I\} = \sum_{i=1}^{L-1} E\{\Re\{\tilde{n}_i^* \tilde{n}_{i-1}\}\} = 0 \quad (22)$$

and

$$\begin{aligned} Var\{X_I\} &= \sum_{i=1}^{L-1} Var\{\Re\{\tilde{n}_i^* \tilde{n}_{i-1}\}\} \\ &\quad + \sum_{i \neq j} Cov\{\Re\{\tilde{n}_i^* \tilde{n}_{i-1}\}, \Re\{\tilde{n}_j^* \tilde{n}_{j-1}\}\} \\ &= 2(L-1)\sigma_n^4. \end{aligned} \quad (23)$$

Similarly, the mean and variance of the quadrature component of X can be determined as 0 and $2(L-1)\sigma_n^4$, respectively. We approximate X as a Gaussian that is the sum of $L-1$ uncorrelated variables, to obtain

$$X_I, X_Q \sim N(0, 2(L-1)\sigma_n^4). \quad (24)$$

Then, $\tilde{Y} = U + V + W + X$ is the sum of the real constant U , the complex Gaussian $V + W$, and X . The complex Gaussian variables $V + W$ and X are uncorrelated since

$$Cov\{V + W, X\} = E\{(V + W)X^*\} = 0 \quad (25)$$

holds. The mean and variance of \tilde{Y} can be obtained by adding the individual mean and variance values indicated in (12), (17), (18), and (24), i.e.,

$$\tilde{Y}_I \sim N(L-1, 2(2L-3)\sigma_n^2 + 2(L-1)\sigma_n^4) \quad (26)$$

and

$$\tilde{Y}_Q \sim N(0, 2\sigma_n^2 + 2(L-1)\sigma_n^4). \quad (27)$$

Thus \tilde{Y}_I^2 follows the *non-central* chi-square distribution with a single degree of freedom with its probability density function (PDF) [10] given by

$$f_{\tilde{Y}_I^2|H_1}(y|H_1) = \frac{\exp\left(-\frac{y+a^2}{2\sigma_{Y_I}^2}\right) \cosh\left(\frac{a\sqrt{y}}{\sigma_{Y_I}^2}\right)}{\sqrt{2\pi y\sigma_{Y_I}^2}}, \quad y \geq 0 \quad (28)$$

where $a = L - 1$ is the non-central parameter and $\sigma_{Y_I}^2 = 2(2L - 3)\sigma_n^2 + 2(L - 1)\sigma_n^4$ is the variance of \tilde{Y}_I . Also, \tilde{Y}_Q^2 follows the *central* chi-square distribution with a single degree of freedom with PDF given by

$$f_{\tilde{Y}_Q^2|H_1}(y|H_1) = \frac{1}{\sqrt{2\pi y\sigma_{Y_Q}^2}} \exp\left(-\frac{y}{2\sigma_{Y_Q}^2}\right), \quad y \geq 0 \quad (29)$$

where $\sigma_{Y_Q}^2 = 2\sigma_n^2 + 2(L - 1)\sigma_n^4$ is the variance of \tilde{Y}_Q .

Since the differential correlation metric in (11) satisfies $S = \tilde{Y}_I^2 + \tilde{Y}_Q^2$, it is the sum of a non-central chi-square variable and a central chi-square variable. Using the result presented in [21, p. 43], we obtain the PDF of S from $f_{\tilde{Y}_I^2|H_1}(y|H_1)$ and $f_{\tilde{Y}_Q^2|H_1}(y|H_1)$, as presented in (30). The corresponding CDF of S is given in (31). These distribution functions include the n th order modified Bessel function of the first kind

$$I_n(x) = \sum_{k=0}^{\infty} \frac{(x/2)^{n+2k}}{\Gamma(k+1)\Gamma(n+k+1)}$$

where

$$\Gamma(\delta) = \int_0^{\infty} t^{\delta-1} \exp^{-t} dt$$

is the Gamma function, and the m th order Marcum Q -function is

$$Q_m(u, v) = \frac{1}{u^{m-1}} \int_v^{\infty} x^m \exp\left(-\frac{x^2+u^2}{2}\right) I_m(ux) dx.$$

Missed detection occurs during frame synchronization when the correlation metric S at the synchronous position does not exceed a given threshold value ξ . The MDP is determined from the derived probability distributions as

$$P_M(\xi) = \int_0^{\xi} f_{S|H_1}(s|H_1) ds = F_{S|H_1}(\xi). \quad (32)$$

B. Asynchronous Case

When $s_i \neq d_i$, variable U does not reduce to a constant value as in the synchronous case. By denoting $U_i = s_i^* s_{i-1} d_i d_{i-1}^*$, we have $U = \sum_{i=1}^{L-1} U_i$. Since each data and synchronization symbol takes a discrete value, U_i is a discrete random variable with its real part following the probability mass function (PMF)

$$P_{\Re\{U_i\}}(x) = (1/4)\delta(x-1) + (1/2)\delta(x) + (1/4)\delta(x+1)$$

where $\delta(\cdot)$ is the Dirac delta function. Using the independent identically distributed Bernoulli random variable Z_i with PMF

$P_{Z_i}(z) = (1/2)\delta(z) + (1/2)\delta(z-1)$, $\Re\{U_i\}$ can be expressed as $\Re\{U_i\} = Z_{2i-1} + Z_{2i} - 1$. Therefore,

$$U_I = \sum_{i=1}^{L-1} \Re\{U_i\} = \sum_{i=1}^{2(L-1)} Z_i - (L-1)$$

follows the binomial distribution with mean $2(L-1) \times 1/2 - (L-1) = 0$ and variance $2(L-1) \times 1/4 = (L-1)/2$. In a similar fashion, U_Q can be shown to follow the binomial distribution with mean 0 and variance $(L-1)/2$. For sufficiently large L , the binomial distribution approaches the Gaussian PDF, so we model U_I and U_Q as

$$U_I, U_Q \sim N(0, (L-1)/2). \quad (33)$$

Variables V and W are uncorrelated and their distributions are separately considered. Each term in variable $V = \sum_{i=1}^{L-1} s_i^* \tilde{n}_{i-1} d_i d_{i-1}^*$ is obtained by rotating the phase of \tilde{n}_{i-1} and follows the identical distribution. Summation of the $L-1$ independent Gaussian terms in V results in in-phase and quadrature components satisfying

$$V_I, V_Q \sim N(0, (L-1)\sigma_n^2), \quad (34)$$

and the distributions for W_I and W_Q are determined as in

$$W_I, W_Q \sim N(0, (L-1)\sigma_n^2). \quad (35)$$

The distribution of variable X is identical for both synchronous and asynchronous cases and is given by

$$X_I, X_Q \sim N(0, 2(L-1)\sigma_n^4) \quad (36)$$

as in (24).

Using individual distributions for the four uncorrelated Gaussian variables U, V, W , and X given in (33)–(36), we observe that the overall distribution of $\tilde{Y} = U + V + W + X$ follows

$$Y_I, Y_Q \sim N(0, (L-1)/2 + 2(L-1)\sigma_n^2 + 2(L-1)\sigma_n^4) \quad (37)$$

where $\sigma_{\tilde{Y}}^2 = (L-1)/2 + 2(L-1)\sigma_n^2 + 2(L-1)\sigma_n^4$ is the variance of both the in-phase and quadrature components of \tilde{Y} . Thus the differential correlation metric $S = \tilde{Y}_I^2 + \tilde{Y}_Q^2$ follows the exponential PDF of

$$f_{S|H_0}(s) = \frac{1}{2\sigma_{\tilde{Y}}^2} \exp\left(-\frac{s}{2\sigma_{\tilde{Y}}^2}\right), \quad s \geq 0 \quad (38)$$

and the corresponding CDF is given by

$$F_{S|H_0}(s|H_0) = 1 - \exp\left(-\frac{s}{2\sigma_{\tilde{Y}}^2}\right), \quad s \geq 0. \quad (39)$$

Erroneous frame boundary detection at asynchronous symbol positions occurs when the correlation metric S exceeds the threshold, and we obtain the FAR using the derived CDF as

$$\begin{aligned} P_F(\xi) &= \int_{\xi}^{\infty} f_{S|H_0}(s|H_0) ds = 1 - F_{S|H_0}(\xi) \\ &= \exp\left(-\frac{\xi}{2\sigma_{\tilde{Y}}^2}\right). \end{aligned} \quad (40)$$

$$f_{S|H_1}(s) = \frac{1}{2\sigma_{Y_I}\sigma_{Y_Q}} \exp\left(-\frac{s+a^2}{2\sigma_{Y_I}^2}\right) \sum_{i=0}^{\infty} \frac{\Gamma(1/2+i)}{\Gamma(i+1)\Gamma(1/2)} \left(\frac{\sqrt{s}(\sigma_{Y_Q}^2 - \sigma_{Y_I}^2)}{a\sigma_{Y_Q}^2}\right)^i I_i\left(\frac{\sqrt{sa}}{\sigma_{Y_I}^2}\right), \quad s \geq 0 \quad (30)$$

$$F_{S|H_1}(s) = \frac{\sigma_{Y_I}}{\sigma_{Y_Q}} \sum_{i=0}^{\infty} \frac{\Gamma(1/2+i)}{\Gamma(i+1)\Gamma(1/2)} \left(\frac{\sigma_{Y_Q}^2 - \sigma_{Y_I}^2}{\sigma_{Y_Q}^2}\right)^i \left(1 - Q_{i+1}\left(\frac{a}{\sigma_{Y_I}}, \frac{\sqrt{s}}{\sigma_{Y_I}}\right)\right), \quad s \geq 0 \quad (31)$$

C. Other Modulation Types

As mentioned in Section II, the distributions obtained for QPSK symbols can easily be extended to other modulation types. For general M -ary PSK, the distributions for V , W , and X remain the same as those for QPSK. The variables defined in (8)–(10) are phase-rotated versions of circularly symmetric noise random variables, so the distributions given in (17), (18), and (24) hold regardless of M . For the synchronous case, variable U has the same constant value $U = L - 1$ using $s_i = d_i$ and $|d_i| = 1$. For the asynchronous case, the discrete random variable U_i follows different PMFs depending on the value of M . When $M = 8$, for example, we obtain

$$P_{\Re\{U_i\}}(x) = (1/8)\delta(x-1) + (1/4)\delta(x-1/\sqrt{2}) + (1/4)\delta(x) + (1/4)\delta(x+1/\sqrt{2}) + (1/8)\delta(x+1)$$

with mean 0 and variance 1/2. For sufficiently large L , both $U_I = \sum_{i=1}^{L-1} \Re\{U_i\}$ and $U_Q = \sum_{i=1}^{L-1} \Im\{U_i\}$ approach the Gaussian PDF, so we model U_I and U_Q as

$$U_I, U_Q \sim N(0, (L-1)/2), \quad (41)$$

which is identical to (33). Although specific PMFs may vary depending on M , the Gaussian model remains the same. In summary, we observe that all the distributions determined for QPSK also apply to general M -PSK.

On the other hand, for M -ary APSK some of the statistics are dependent upon a given pattern of the synchronization sequence. Let us define $\alpha = \sum_{i=1}^{L-1} |d_i|^2 |d_{i-1}|^2 / (L-1)$, $\beta = (|d_0|^2 + |d_{L-1}|^2 + 4 \sum_{i=1}^{L-2} |d_i|^2) / (4L-6)$, and $\gamma = (|d_0|^2 + |d_{L-1}|^2) / 2$, which are determined by the specific synchronization sequence symbols $\{d_i\}$. Note that $\alpha = \beta = \gamma = 1$ for the PSK symbols. Using these parameters and following a similar derivation procedure, the distributions for M -APSK can be obtained as follows.

Synchronous case: We have $U = \sum_{i=1}^{L-1} |d_i|^2 |d_{i-1}|^2 = \alpha(L-1)$ and the real and imaginary parts of $V+W$ follow

$$V_I + W_I \sim N(0, \beta(4L-6)\sigma_n^2) \quad \text{and} \quad V_Q + W_Q \sim N(0, 2\gamma\sigma_n^2).$$

Also, since the real and imaginary parts of X follow

$$X_I, X_Q \sim N(0, 2\alpha(L-1)\sigma_n^4),$$

the distributions in (26) and (27) change to

$$\tilde{Y}_I \sim N(\alpha(L-1), \beta(4L-6)\sigma_n^2 + 2\alpha(L-1)\sigma_n^4)$$

and

$$\tilde{Y}_Q \sim N(0, 2\gamma\sigma_n^2 + 2\alpha(L-1)\sigma_n^4).$$

Asynchronous case: From $E\{s_i^*\} = 0$ and $E\{|s_i|^2\} = 1$, we have $E\{U_i\} = 0$ and $\text{Var}\{U_i\} = |d_i|^2 |d_{i-1}^*|^2$. Applying the central limit theorem for sufficiently large L , the distributions of real and imaginary parts of U are given by

$$U_I, U_Q \sim N(0, \alpha(L-1)/2).$$

The real and imaginary parts of V and W follow the distribution

$$V_I, V_Q, W_I, W_Q \sim N(0, \alpha(L-1)\sigma_n^2)$$

and the distribution for variable X is determined as

$$X_I, X_Q \sim N(0, 2\alpha(L-1)\sigma_n^4).$$

Hence, the distributions for Y_I and Y_Q in (37) change to

$$Y_I, Y_Q \sim N(0, \alpha(L-1)(1/2 + 2\sigma_n^2 + 2\sigma_n^4)).$$

IV. EXTENSION TO MULTI-SPAN DIFFERENTIAL CORRELATION

Generalizing the expression in (6), the k -span differential correlation $Y(k)$ in (4) can be written as

$$Y(k) = e^{-j2\pi k f_0 T_s} [U(k) + V(k) + W(k) + X(k)] \quad (42)$$

where

$$U(k) \triangleq \sum_{i=k}^{L-1} s_i^* s_{i-k} d_i d_{i-k}^*, \quad (43)$$

$$V(k) \triangleq \sum_{i=k}^{L-1} s_i^* \tilde{n}_{i-k} d_i d_{i-k}^*, \quad (44)$$

$$W(k) \triangleq \sum_{i=k}^{L-1} \tilde{n}_i^* s_{i-k} d_i d_{i-k}^*, \quad \text{and} \quad (45)$$

$$X(k) \triangleq \sum_{i=k}^{L-1} \tilde{n}_i^* \tilde{n}_{i-k} d_i d_{i-k}^*. \quad (46)$$

The multi-span correlation metric in (5) is given by

$$S = \sum_{k=1}^K |U(k) + V(k) + W(k) + X(k)|^2 = \sum_{k=1}^K |\tilde{Y}(k)|^2 + \sum_{k=1}^K \{\tilde{Y}_I^2(k) + \tilde{Y}_Q^2(k)\} \quad (47)$$

where $\tilde{Y}(k) \triangleq U(k) + V(k) + W(k) + X(k)$.

A. Synchronous Case

The distributions for $U(k)$, $V(k)$, $W(k)$, and $X(k)$ can be obtained by a procedure similar to the derivation of the single-span correlation distributions in Section III. Using $s_i = d_i$, variable $U(k)$ becomes

$$U(k) = L - k. \quad (48)$$

From $\text{Var}\{V_I(k) + W_I(k)\} = (2 + 4(L - 1 - k))\sigma_n^2$ and $\text{Var}\{V_Q(k) + W_Q(k)\} = 2\sigma_n^2$, the in-phase and quadrature components of $V(k) + W(k)$ follow

$$V_I(k) + W_I(k) \sim N(0, 2(2L - 2k - 1)\sigma_n^2) \quad (49)$$

and

$$V_Q(k) + W_Q(k) \sim N(0, 2\sigma_n^2). \quad (50)$$

Further, the distribution of $X(k)$ is approximated as

$$X_I(k), X_Q(k) \sim N(0, 2(L - k)\sigma_n^4). \quad (51)$$

Then, the distribution of Y_I , the sum of uncorrelated variables $U(k)$, $V(k) + W(k)$, and $X(k)$, can be expressed by

$$Y_I(k) \sim N(L - k, 2(2L - 2k - 1)\sigma_n^2 + 2(L - k)\sigma_n^4) \quad (52)$$

and

$$Y_Q(k) \sim N(0, 2\sigma_n^2 + 2(L - k)\sigma_n^4). \quad (53)$$

B. Asynchronous Case

Following the same procedure for the derivation for the asynchronous single-span correlation except with the summation limit for variables $U(k)$, $V(k)$, $W(k)$, and $X(k)$ changed from $L - 1$ to $L - k$, we obtain the distribution of $Y(k)$ as

$$Y_I(k), Y_Q(k) \sim N(0, (L - k)/2 + 2(L - k)\sigma_n^2 + 2(L - k)\sigma_n^4). \quad (54)$$

Note that for the asynchronous case, variables $Y(i)$ and $Y(j)$, $i \neq j$, are uncorrelated, whereas statistical dependency exists between these variables in the synchronous case.

C. Special Case: $K = 2$

When $K = 2$, the correlation metric becomes

$$S = Y_I^2(1) + Y_Q^2(1) + Y_I^2(2) + Y_Q^2(2). \quad (55)$$

For the synchronous case, the means of $Y_I^2(k)$ and $Y_Q^2(k)$ are

$$\begin{aligned} E\{Y_I^2(k)\} &= \text{Var}\{Y_I(k)\} + (E\{Y_I(k)\})^2 \\ &= 2(2L - 2k - 1)\sigma_n^2 + 2(L - k)\sigma_n^4 + (L - k)^2 \end{aligned}$$

and

$$\begin{aligned} E\{Y_Q^2(k)\} &= \text{Var}\{Y_Q(k)\} + (E\{Y_Q(k)\})^2 \\ &= 2\sigma_n^2 + 2(L - k)\sigma_n^4. \end{aligned}$$

We observe that the relation $E\{Y_I^2(k)\} \gg E\{Y_Q^2(k)\}$ holds for a sufficiently large value of L , so we approximate the metric by

$$S \approx Y_I^2(1) + Y_I^2(2) \quad (56)$$

under the large L assumption. Although there exists statistical correlation between $Y_I^2(1)$ and $Y_I^2(2)$, we derive the distribution of S by assuming the independence of these two random variables. The PDF and CDF of S are obtained and presented in (57) and (58), where $a_k = L - k$ is the non-centrality parameter and $\sigma_{Y_k}^2 = 2(2L - 2k - 1)\sigma_n^2 + 2(L - k)\sigma_n^4$. The MDP is computed using the CDF of

$$P_M(\xi) = F_{S|H_1}(\xi|H_1). \quad (59)$$

For the asynchronous case, the metric is the sum of two independent central chi-square variables with two degrees of freedom, and the exact PDF can be determined. We obtain

$$f_{S|H_0}(s) = \frac{\exp\left(-\frac{s}{2\sigma_{Y_2}^2}\right) - \exp\left(-\frac{s}{2\sigma_{Y_1}^2}\right)}{2(\sigma_{Y_2}^2 - \sigma_{Y_1}^2)}, \quad s \geq 0 \quad (60)$$

and the corresponding CDF is

$$\begin{aligned} F_{S|H_0}(s) &= 1 - \left(\frac{\sigma_{Y_2}^2}{\sigma_{Y_2}^2 - \sigma_{Y_1}^2}\right) \exp\left(-\frac{s}{2\sigma_{Y_2}^2}\right) \\ &\quad + \left(\frac{\sigma_{Y_1}^2}{\sigma_{Y_2}^2 - \sigma_{Y_1}^2}\right) \exp\left(-\frac{s}{2\sigma_{Y_1}^2}\right), \quad s \geq 0 \end{aligned} \quad (61)$$

where $\sigma_{Y_k}^2 = (L - k)/2 + 2(L - k)\sigma_n^2 + 2(L - k)\sigma_n^4$. The probability that frame synchronization is erroneously made at asynchronous positions can be obtained by evaluating the FAR of

$$P_F(\xi) = 1 - F_{S|H_0}(\xi). \quad (62)$$

The exact distribution for the sum of K non-central chi-square random variables that are correlated is unknown for $K > 2$ [21]. Thus closed-form expressions for error probabilities for general K are not presented in this paper, and one may have to resort to simulated results for performance evaluation.

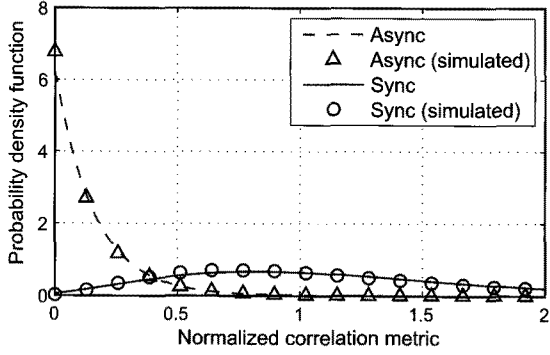
V. NUMERICAL RESULTS

The derived formulas are evaluated using different numerical parameters. We use $E_s/N_0 = 0, 5$, and 10 dB representing low, medium, and high channel SNR values; $L = 26, 50$, and 100 representing short, medium, and long correlation lengths are tested separately. $L = 26$ corresponds to the header synchronization sequence length for the current DVB-S2 standard [1], and the use of longer synchronization sequences to guarantee rapid re-synchronization for hostile channel conditions is also under consideration [22].

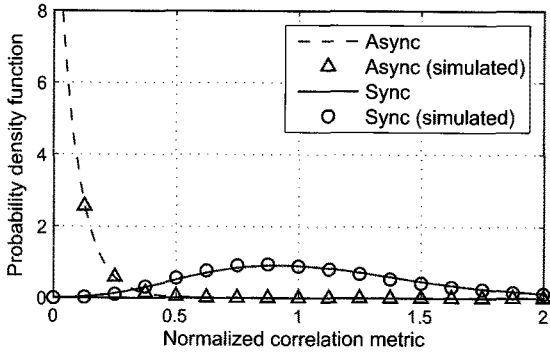
The PDFs of S are plotted in Fig. 2 for the synchronous case using (30) and the asynchronous case using (38) at 0 dB SNR. The metric value is normalized such that the metric for the synchronous correlation becomes unity in the absence of noise, by dividing the metric by the squared non-centrality parameter $a^2 = (L - 1)^2$. The distributions for the synchronous and asynchronous cases are denoted by the solid and dashed lines, respectively, and the two distributions are shown to have

$$f_{S|H_1}(s) = \frac{\exp\left(-\frac{s + a_1^2}{2\sigma_{Y_1}^2} - \frac{a_2^2}{2\sigma_{Y_2}^2}\right)}{2\sigma_{Y_1}\sigma_{Y_2}} \sum_{i=0}^{\infty} \sum_{l=0}^{\infty} \frac{\Gamma(1/2 + i + l)}{i!l!\Gamma(1/2 + l)} \left(\frac{\sqrt{s}a_2\sigma_{Y_1}^2}{2a_1\sigma_{Y_2}^2}\right)^l \left(\frac{\sqrt{s}(\sigma_{Y_2}^2 - \sigma_{Y_1}^2)}{a_1\sigma_{Y_2}^2}\right)^i I_{i+l}\left(\frac{\sqrt{s}a_1}{\sigma_{Y_1}^2}\right), \quad s \geq 0 \quad (57)$$

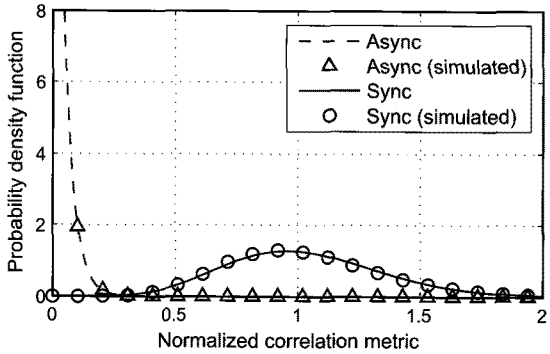
$$F_{S|H_1}(s) = \frac{\sigma_{Y_1}}{\sigma_{Y_2}} \exp\left(-\frac{a_2^2}{2\sigma_{Y_2}^2}\right) \sum_{i=0}^{\infty} \sum_{l=0}^{\infty} \frac{\Gamma(1/2 + i + l)}{i!l!\Gamma(1/2 + l)} \left(\frac{a_2^2\sigma_{Y_1}^2}{2\sigma_{Y_2}^2}\right)^l \left(\frac{\sigma_{Y_2}^2 - \sigma_{Y_1}^2}{\sigma_{Y_2}^2}\right)^i \left(1 - Q_{i+l+1}\left(\frac{a_1}{\sigma_{Y_1}}, \frac{\sqrt{s}}{\sigma_{Y_1}}\right)\right), \quad s \geq 0 \quad (58)$$



(a)



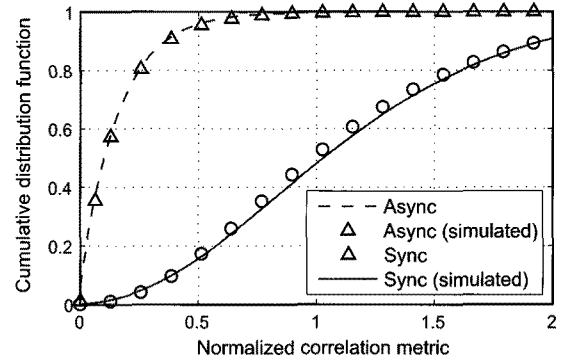
(b)



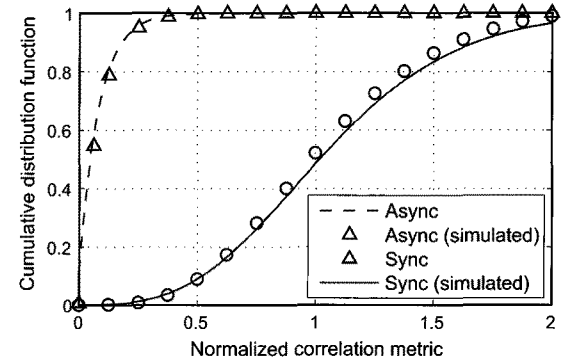
(c)

Fig. 2. PDFs of the differential correlation metric with varying correlation lengths at 0 dB SNR: (a) $L = 26$, (b) $L = 50$, and (c) $L = 100$.

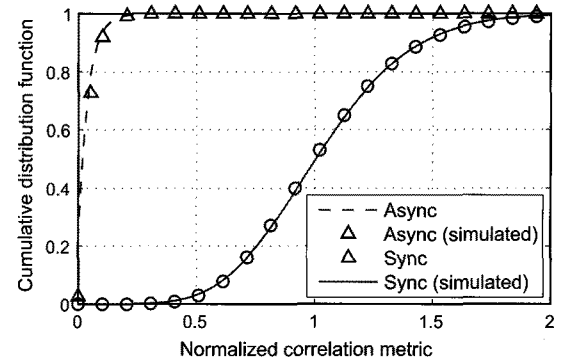
a wider separation as the correlation length increases, resulting in improved detection performance. In the figure, the analytic distributions are compared with simulation results, obtained by repeated generations of the correlation metric using a noise-corrupted synchronization sequence and data symbols.



(a)



(b)



(c)

Fig. 3. CDFs of the differential correlation metric with varying correlation lengths at 0 dB SNR: (a) $L = 26$, (b) $L = 50$, and (c) $L = 100$.

The maximum frequency offset corresponding to 20% of the transmission bandwidth is applied, i.e., the frequency offset is uniformly generated from the range $[-0.2/T_s, +0.2/T_s]$. Since the correlation property of specific synchronization sequences is not important in this study, the simulation uses random binary code patterns for the synchronization symbols. Although some

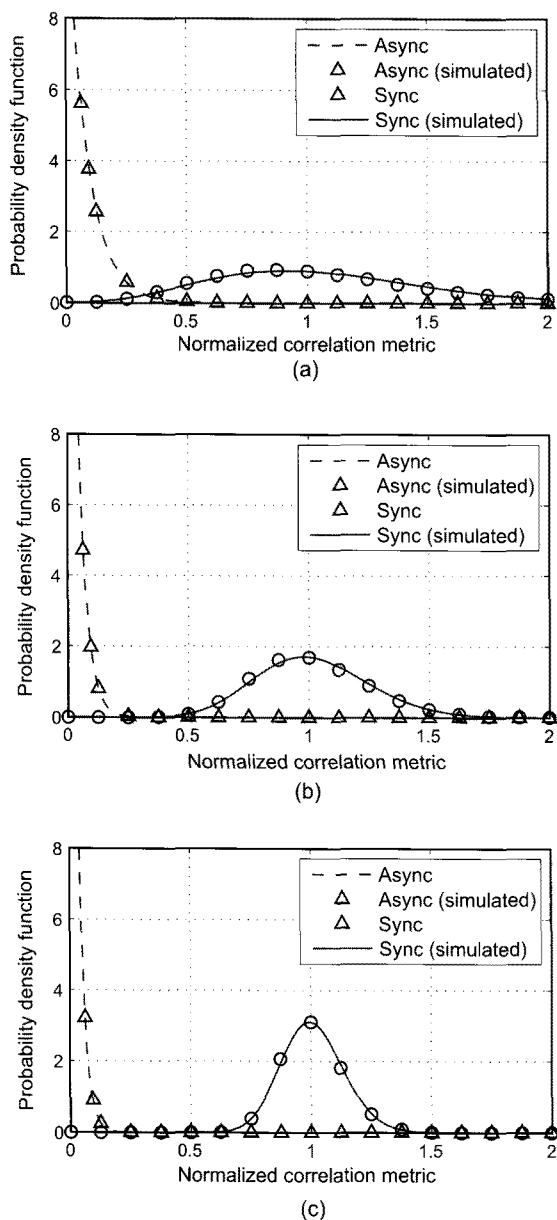


Fig. 4. PDFs of the differential correlation metric with varying channel SNR values ($L = 50$): (a) SNR = 0 dB, (b) SNR = 5 dB, and (c) SNR = 10 dB.

of the approximations used in the analysis are more applicable when the correlation length increases, the figure shows that the derived formulas are in good agreement with the experimental values for all correlation lengths tested.

Fig. 3 shows the changes in the PDFs for different SNR values, indicating that the variance of the distributions reduces rapidly as SNR increases. Since the error probabilities are functions of the threshold value, the MDP and FAR can be determined for different threshold values as shown in Fig. 4. Finally, Fig. 5 shows the multi-span differential correlation statistics obtained from the analytic expressions in (57) and (60).

As mentioned in Sections III and IV, several approximations were made to determine the probability distributions. A key approximation is modeling the sums of random variables as Gaussian, including variable X in (24) and (36) for both

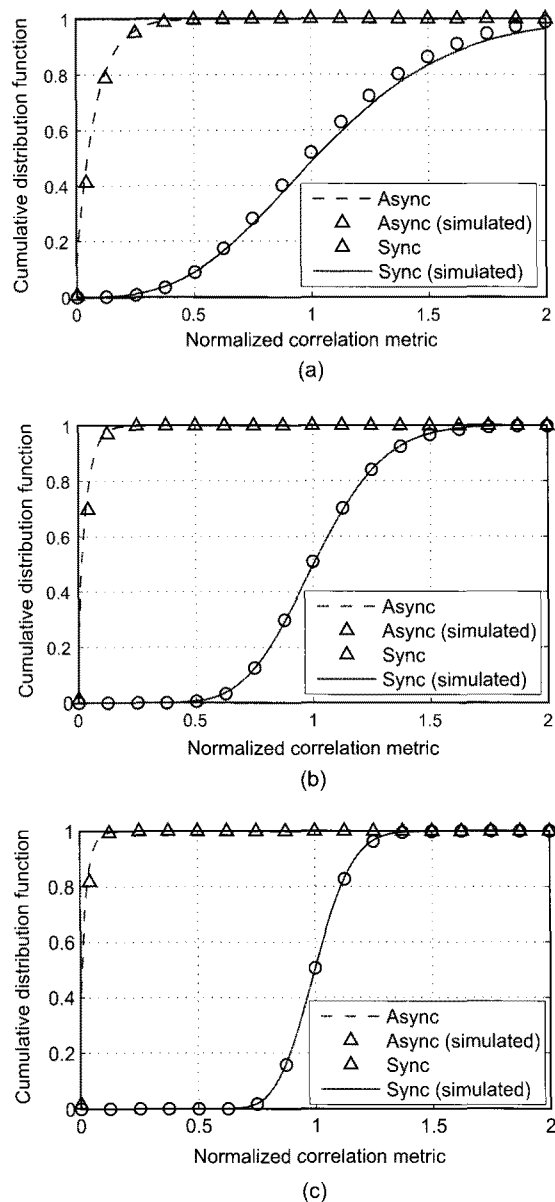


Fig. 5. CDFs of the differential correlation metric with varying channel SNR values ($L = 50$): (a) SNR = 0 dB, (b) SNR = 5 dB, and (c) SNR = 10 dB.

the synchronous and asynchronous cases, and the sum of binomial variables U in (33). Another approximation, as indicated in (56), is using the dominance of the in-phase component of Y for large L . These approximations become more accurate as the synchronization sequence length increases. In fact, the presented formulas are shown to be quite accurate even for moderate lengths, e.g., $L \geq 26$ as demonstrated in Figs. 2 to 5. The final approximation is the assumption of independence between variables $Y(1)$ and $Y(2)$ in the derivation of (57) for the synchronous multi-span correlation. This approximation has resulted in a slight offset between formula and experiment, as shown in Figs. 7 and 8. Note that variables $Y(1)$ and $Y(2)$ are independent in the asynchronous case and no further assumption was necessary for the derivation of (60). This is also confirmed by the exact match of formula and experiment for the asynchronous case in the same figures.

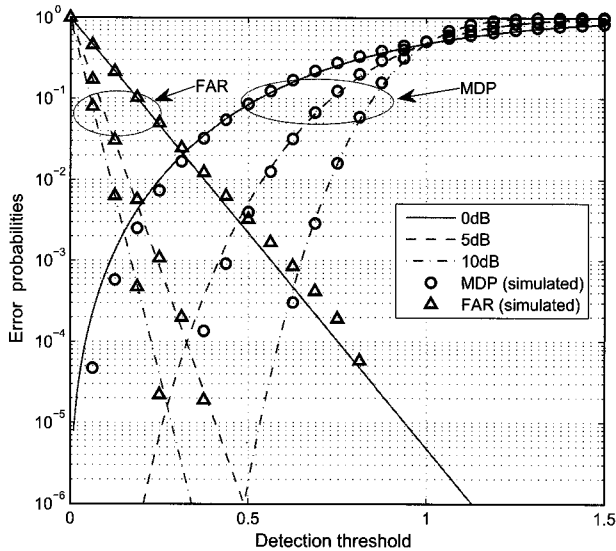


Fig. 6. Mis-detection probabilities and false alarm rates for frame synchronization using differential correlation ($L = 50$).

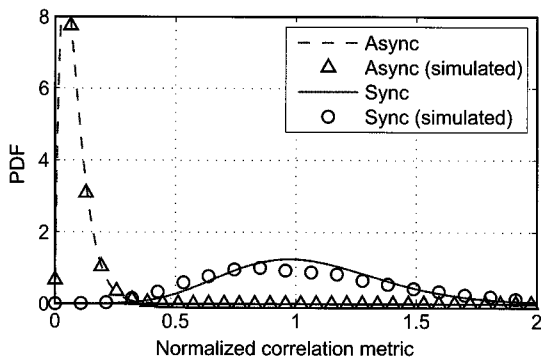


Fig. 7. PDFs of the differential correlation metric using the double-span correlations at 0 dB SNR ($L = 50$).

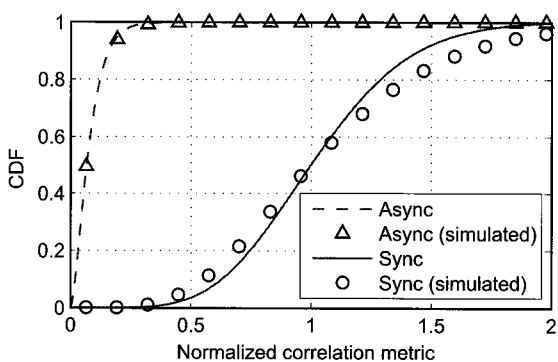


Fig. 8. CDFs of the differential correlation metric using the double-span correlations at 0 dB SNR ($L = 50$).

One final comment is on the numerical computation of the MDP formulas for the synchronous case. Although the formulas involve an infinite sum of Gamma and Marcum Q -functions as indicated in (31), the actual computation is performed over a finite range of the summation index because of the fast conver-

gence behavior of the sum. In many cases, the first few terms dominate the MDP value, and all the results in this paper used no more than ten leading terms since virtually no change occurs with the inclusion of more terms.

VI. CONCLUSIONS

We have investigated probabilistic modeling of the differential correlation output and presented analytic expressions for its distributions. At synchronous positions, the PDF is expressed in terms of multi-order Bessel functions, while the asynchronous distribution is represented by simple exponential functions. Since the distribution functions determine the detection error probabilities, our formulas are applicable for predicting the performance of frame synchronization using differential correlators under various channel conditions.

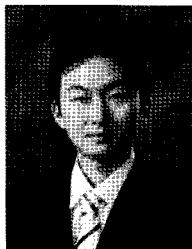
REFERENCES

- [1] "Digital video broadcasting (DVB): Second generation framing structure, channel coding and modulation system for broadcasting, interactive services, news gathering and other broadband satellite applications," ETSI EN 302 307 v1.1.1, June 2004.
- [2] U. Reimers, "DVB - The family of international standards for digital video broadcasting," *Proc. IEEE*, vol. 94, pp. 173-182, Jan. 2006.
- [3] A. Morello, "DVB-S2: The second generation standard for satellite broadband services," *Proc. IEEE*, vol. 94, pp. 210-227, Jan. 2006.
- [4] E. Casini, R. De Gaudenzi, and A. Ginesi, "DVB-S2 modem algorithms design and performance over typical satellite channels," *Int. J. Satellite Commun. Network.*, vol. 22, no. 3, pp. 281-318, May/June 2004.
- [5] J. L. Massey, "Optimum frame synchronization," *IEEE Trans. Commun.*, vol. 20, pp. 115-119, Apr. 1972.
- [6] P. T. Nielsen, "Some optimum and suboptimum frame synchronizers for binary data in Gaussian noise," *IEEE Trans. Commun.*, vol. 21, pp. 770-772, June 1973.
- [7] G.-G. Bi, "Performance of frame sync acquisition algorithms on the AWGN channel," *IEEE Trans. Commun.*, vol. 31, pp. 1196-1201, Oct. 1983.
- [8] G. L. Lui and H. H. Tan, "Frame synchronization for Gaussian channels," *IEEE Trans. Commun.*, vol. 35, pp. 818-829, Aug. 1987.
- [9] J. A. Gansman, M. P. Fitz, and J. V. Krogmeier, "Optimum and suboptimum frame synchronization for pilot-symbol-assisted modulation," *IEEE Trans. Commun.*, vol. 45, pp. 1327-1337, Oct. 1997.
- [10] J. G. Proakis, *Digital Communications*, 4th ed. New York: McGraw-Hill, 2001.
- [11] D. E. Cartier, "Partial correlation properties of pseudonoise (PN) codes in noncoherent synchronization/detection schemes," *IEEE Trans. Commun.*, vol. 24, pp. 898-903, Aug. 1976.
- [12] J. Diez, C. Pantaleon, L. Vielva, I. Santamaria, and J. Ibanez, "A simple expression for the optimization of spread-spectrum code acquisition detectors operating in the presence of carrier-frequency offset," *IEEE Trans. Commun.*, vol. 52, pp. 550-552, Apr. 2004.
- [13] Z. Y. Choi and Y. H. Lee, "Frame synchronization in the presence of frequency offset," *IEEE Trans. Commun.*, vol. 50, pp. 1062-1065, July 2002.
- [14] S. Park, D. Park, H. Park, and K. Lee, "Low-complexity frequency-offset insensitive detection for orthogonal modulation," *Electron. Lett.*, vol. 41, pp. 1226-1228, Oct. 2005.
- [15] P. Kim, G. E. Corazza, R. Pedone, M. Villanti, D.-I. Chang, and D. Oh, "Enhanced frame synchronization for DVB-S2 system under a large of frequency offset," in *Proc. IEEE WCNC*, Mar. 2007, pp. 1183-1187.
- [16] G. E. Corazza and R. Pedone, "Generalized and average likelihood ratio testing for post detection integration," *IEEE Trans. Commun.*, vol. 55, pp. 2159-2171, Nov. 2007.
- [17] M. Villanti, P. Salmi, and G. E. Corazza, "Differential post-detection integration techniques for robust code acquisition," *IEEE Trans. Commun.*, vol. 55, pp. 2172-2184, Nov. 2007.
- [18] R. Pulikoonattu and M. Antweiler, "Analysis of differential non coherent detection scheme for CDMA pseudo random (PN) code acquisition," in *Proc. IEEE ISSSTA*, Sept. 2004, pp. 212-217.
- [19] R. Pulikoonattu, P. K. Venkataraghavan, and T. Ray, "A modified non-coherent PN code acquisition scheme," in *Proc. IEEE WCNC*, Mar. 2004, pp. 1568-1571.

- [20] A. Schmid and A. Neubauer, "Differential correlation for Galileo/GPS receivers," in *Proc. IEEE ICASSPs*, Mar. 2005, pp. 953–956.
- [21] M. K. Simon, *Probability Distributions Involving Gaussian Random Variables*. Boston: Kluwer, 2002.
- [22] ETSI S2M.r2, *Draft Baseline S2 System for Mobility*, July 2006.
- [23] H. L. Van Trees, *Detection, Estimation, and Modulation Theory – Part I*. New York: Wiley, 1968.
- [24] J. Hu and N. C. Beaulieu, "Accurate simple closed-form approximations to Rayleigh sum distributions and densities," *IEEE Commun. Lett.*, vol. 9, pp. 109–111, Feb. 2005.
- [25] G. K. Karagiannidis, T. A. Tsiftsis, and N. C. Sagias, "A closed-form upper-bound for the distribution of the weighted sum of Rayleigh variates," *IEEE Commun. Lett.*, vol. 9, pp. 589–591, July 2005.
- [26] D. A. Shnidman, "Two noncentral chi-square generalizations," *IEEE Trans. Inform. Theory*, vol. 42, pp. 283–285, Jan. 1996.
- [27] C.-S. Kim, D.-J. Oh, and L. B. Milstein, "Statistical modeling of W-CDMA signals for use over frequency-selective multipath channels," *IEEE Trans. Commun.*, vol. 52, pp. 28–30, Jan. 2004.
- [28] D. A. Shnidman, "Generalized radar clutter model," *IEEE Trans. Aerosp. Electron. Syst.*, vol. 35, pp. 857–865, July 1999.
- [29] D. A. Shnidman, "Radar detection probabilities and their calculation," *IEEE Trans. Aerosp. Electron. Syst.*, vol. 31, pp. 928–950, July 1995.



Sangtae Kim was born in Seoul, Korea, in March 10, 1980. He received his B.S. and M.S. degrees in Electronics Engineering from Sogang University, Seoul, Korea in 2006 and 2008, respectively. He is currently with the Modem S/W Research Team, DMC R& D Center, Samsung Electronics Co. His research interests include statistical analysis of communication systems, mobile wireless systems, and satellite modems. He received the Best Paper Award from the 18th Joint Conference on Communications and Information held in Jeju, Korea in April 2008.



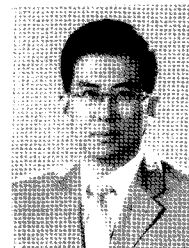
Jaewon Kim was born in Seoul, Korea, on November 10, 1981. He received the B.S. and M.S. degrees in Electronic Engineering from Sogang University, Seoul, Korea in 2007 and 2009, respectively. He is currently pursuing his Ph.D. degree at Sogang University. His research interests include statistic analysis, communication signal processing, space-time coding, and multi-user MIMO systems. He is a co-recipient of the Best Paper Award from the 18th Joint Conference on Communications and Information held in Jeju, Korea in April 2008.



Dong-Joon Shin received the B.S. degree in Electronics Engineering from Seoul National University, Seoul, Korea, the M.S. degree in Electrical Engineering from Northwestern University, Evanston, IL, and the Ph.D. degree in Electrical Engineering from University of Southern California, Los Angeles, CA. From 1999 to 2000, he was a Member of Technical Staff in Wireless Network Division and Satellite Network Division, Hughes Network Systems, Germantown, MD. Since September 2000, he has been an Associate Professor in the Department of Electronic Engineering at Hanyang University, Seoul, Korea. His current research interests include digital communication systems, error-correcting codes, sequences, and discrete mathematics.



Dae-Ig Chang received his B.S. and M.S. degrees in Electronics and Telecommunications Engineering from Hanyang University, Seoul, Korea, in 1985 and 1989, respectively, and Ph.D. degree in Electronics Engineering from Chungnam National University in 1999. Since February 1990, he has worked in Satellite Broadcast and Telecommunications Convergence Research Team of ETRI as a Team Leader and Principal Research Staff. From June 1991 to July 1993, he worked as a Member of Research Staff with MPR Teltech Ltd, Vancouver, Canada, where he was involved in developing VSAT systems. Since February 2005, he has been an Adjunct Professor in Mobile Communication and Digital Broadcasting Engineering, University of Science and Technology, Daejeon, Korea. His research interests are digital communications, broadband satellite broadcasting systems, channel adaptive digital modem design, and channel coding.



Wonjin Sung received his B.S. degree from Seoul National University, Korea in 1990, and the M.S. and Ph.D. degrees in Electrical Engineering from University of Michigan, Ann Arbor, MI, in 1992 and 1995, respectively. From January 1996 through August 2000, he worked at Hughes Network Systems, Germantown, MD, USA, where he participated in development projects for cellular and satellite systems including IS-136 base station modems, multi-mode ground terminals for medium orbit satellites, and Inmarsat-IV system air interface design. Since September 2000, he has been with the Department of Electronic Engineering at Sogang University, Seoul, Korea, where he is currently a Professor. His research interests are in the areas of mobile wireless transmission, statistical communication theory, distributed antenna systems, and satellite modems.